Proceedings of the International School of Physics "Enrico Fermi"
Course 197 "Foundations of Quantum Theory", edited by E. M. Rasel, W. P. Schleich and S. Wölk
(IOS, Amsterdam; SIF, Bologna) 2019
DOI 10.3254/978-1-61499-937-9-285

Quantum imaging

Robert W. Boyd

Department of Physics and School of Electrical Engineering and Computer Science
University of Ottawa - Ottawa, Ontario, K1N 6N5 Canada

The Institute of Optics and Department of Physics and Astronomy
University of Rochester - Rochester, New York, 14627 USA

School of Physics and Astronomy, University of Glasgow - Glasgow G12 8QQ, UK

Summary. — We present a brief overview of the field of quantum imaging, concentrating on some recent results. Quantum imaging is a specific example of quantum metrology, and we thus start out with a discussion of quantum metrology including the generation of squeezed light and the generation of entangled photon pairs through the process of spontaneous parametric downconversion (SPDC). We then proceed to review three different examples of quantum imaging, namely ghost imaging, imaging based on interaction-free measurements, and imaging based on Mandel's induced coherence.

1. – What is quantum imaging?

The goal of quantum imaging is to produce "better" images using quantum methods. These images can be better in that they are created through use of a very small number of photons, that they possess better spatial resolution, or that the possess a better signal-to-noise ratio. From a more abstract point of view, one can say that quantum imaging is image formation that exploits the quantum properties of the transverse structure of light fields. In this paper, we present a review of some recent work on this topic. A good summary of earlier work is presented in the book Quantum Imaging [1].

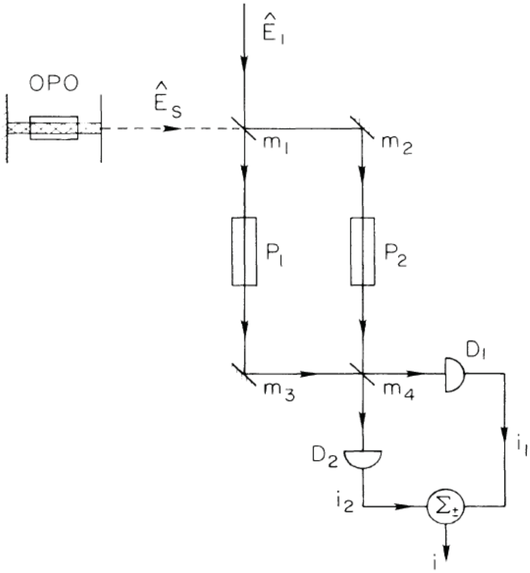

Fig. 1. – Laboratory setup for the demonstration of sub-shot-noise sensitivity through use of squeezed light [4].

2. – Brief history of quantum methods in metrology

Before turning our attention to quantum imaging, it is instructive to first review the usefulness of quantum methods more generally for their use in metrology. Under proper conditions, quantum methods allow one to perform optical measurements with an accuracy that exceeds the "standard quantum limit", the limit imposed by shot noise in a measurement apparatus.

One example of a quantum method in metrology is the use of squeezed light [2]. Squeezed light refers to a light field in which the fluctuations in one conjugate variable are suppressed at the expense of having increased fluctuations in the other conjugate variable. One specific example of squeezed light is quadrature-squeezed light, in which the fluctuations of one quadrature of the field (the part oscillating as $\cos \omega t$, for example) are suppressed and the fluctuations in the other quadrature (the part oscillating as $\sin \omega t$) are increased. Certain nonlinear optical interactions can create light fields with this squeezing property. Quadrature-squeezed light was first demonstrated by the group of Slusher in 1985 [3]. Its application to precision metrology was demonstrated by the group of Kimble [4]. The experimental setup of this work is shown in fig. 1. P_1 and P_2 represent phase modulators placed inside a Mach-Zehnder interferometer. These devices represent the phase objects to be measured by the interferometer. The input to the interferometer is provided by a coherent laser beam E_1 and from the squeezed-vacuum output of an optical parametric oscillator (OPO). Some of the measured results are shown in fig. 2.

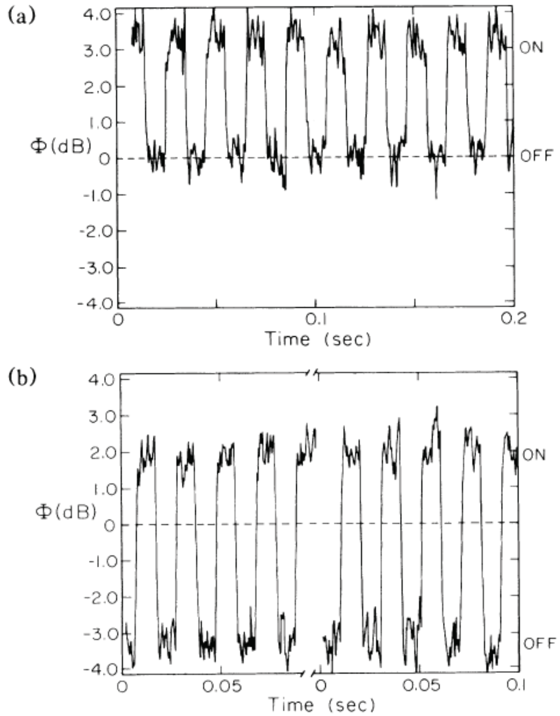

Fig. 2. – Example of data collected with the setup of fig. 1 [4].

The top right figure shows the noise in the output when the OPO is blocked so that the (fluctuating) electromagnetic vacuum enters through the left port. In obtaining this trace, phase modulator P_1 is modulated at 50 Hz to vary the output power. The dashed line at $\Phi = 0$ shows the standard quantum limit (shot noise level). The bottom right figure shows the noise level when the OPO is unblocked so that squeezed vacuum is injected into the left port. One sees that the noise level is decreased by approximately 3 dB. This decreased noise level allows one to make more accurate measurements of any phase shift between the two arms of the interferometer.

Another example of quantum methods in metrology is afforded through use of twin beams. Twin beams are beams of light that contain identical fluctuations. Therefore, although each beam is "noisy", the difference in the intensities of the beams has greatly reduced noise and in principle is entirely noise free. Quantum metrology based on twin beams has been studied extensively by the group of Fabre and coworkers [5]. One example is shown in fig. 3. Here one of the beams falls passes through a potassium vapor cell and is detected by DET2. Its twin falls directly onto detector DET1. The difference in the two photocurrents is measured and is plotted in fig. 4 as a function of the frequency of the light. The trace on the left is seen to be much less noisy than the trace on the right obtained without the use of twin beams.

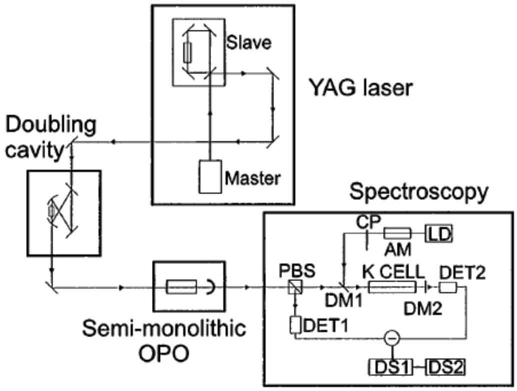

Fig. 3. – Laboratory setup for the demonstration of sub-shot-noise sensitivity through the use of twin beams [5].

Another quantum resource of considerable interest in metrology and in quantum technologies is afforded by entangled light fields. Applications of entangled light fields include quantum teleportation and quantum cryptography. Entangled light sources are also used for performing fundamental tests of quantum mechanics, such as its inherent nonlocality as illustrated in Einstein-Podolsky-Rosen correlations. In the next section, we review one of the standard means of generating entangled photon pairs.

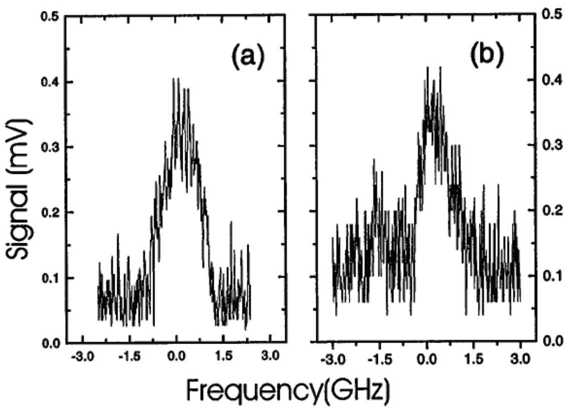

Fig. 4. – Demonstration of sub-shot-noise sensitivity using the setup of fig. 3 [5].

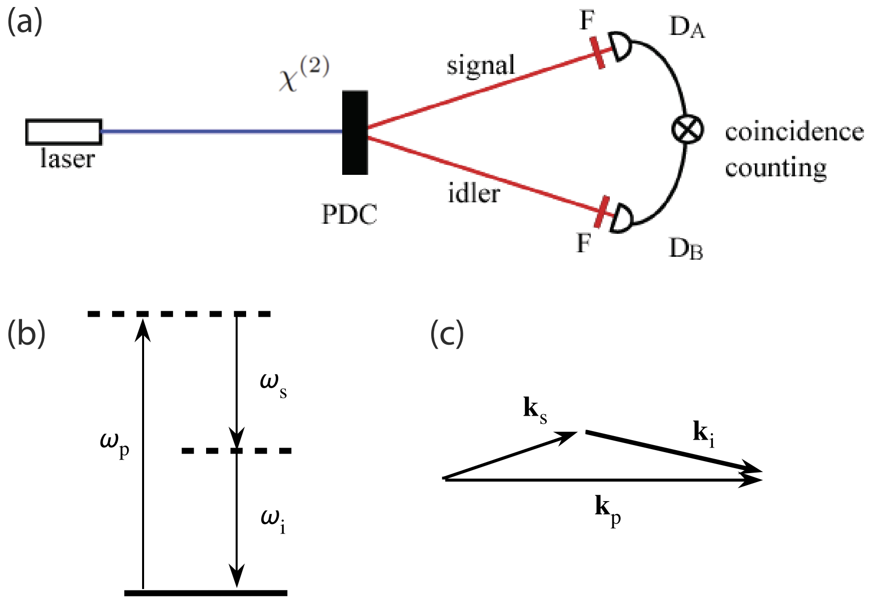

Fig. 5. – (a) Process of parametric downconversion (PDC). (b) Energy conservation in PDC. (c) Wave vector conservation in PDC.

3. – Parametric downconversion and the generation of entangled photons

A primary method for the creation of entangled photons is through the process of parametric downconversion (PDC). This process is illustrated in fig. 5. Part (a) of the figure shows an intense laser beam illuminating a crystal characterized by a second-order nonlinear optical response. On occasion a pump photon splits into two new photons as a consequence of the nonlinear response of the system. For historical reasons these two photons are known as the signal and idler photon, with considerable arbitrariness as to which photon is the signal and which is the idler. Part (b) of the figure illustrates this process in terms of an energy-level diagram, and part (c) shows how photon momentum is conserved in this process.

The photon pairs created by this process are said to be entangled, and they can show entanglement by means of any of their degrees of freedom, such as (a) polarization, (b) time and energy, (c) position and transverse momentum, or (d) angular position and orbital angular momentum. As an example of what is meant by entanglement, we consider the specific case of time-energy entanglement. The photons created by the PDC process of fig. 5 have the property that if the signal frequency ω_s is measured, then one can immediately predict that the idler frequency is given by $\omega_i = \omega_p - \omega_s$. However, if instead of measuring the frequency of the signal photon, one measures the moment of time when it was created, one always finds that the idler photon was created at the same moment of time. However, by measuring the moment of time when the signal photon

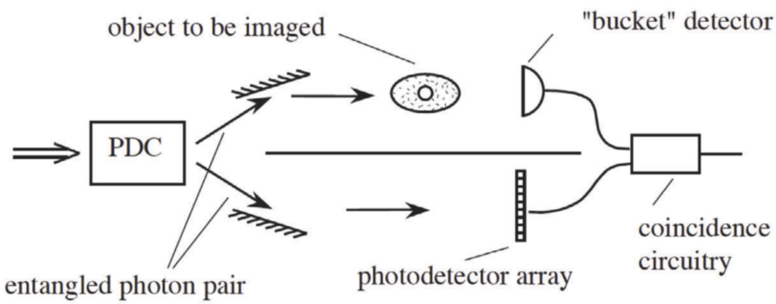

Fig. 6. – Illustration of the process of ghost imaging.

was created, one loses all knowledge of its energy, and in fact one even loses all knowledge of the energy of the idler photon. Likewise, when one measures the energy of the signal photon, one loses all knowledge of the emission time of both signal and idler photons. In fact, one can wait until both photons have long left the crystal and become well separated from one another before deciding which property (energy or emission time) of the signal photon to measure. Nonetheless, the idler photon is always found to have the same property perfectly correlated with that of the signal photon. This property is the key experimental signature of entanglement: the two photons have properties that are completely correlated even in two mutually unbiased bases.

4. – What is ghost imaging and what are its properties?

Ghost imaging, also known as coincidence imaging, is a special sort of imaging technique that can offer significant advantages under certain circumstances. Ghost imaging was originally reported by Strekalov *et al.* [6] and by Pittman *et al.* [7] and has subsequently been studied by many groups [8-20].

The process of ghost imaging is shown schematically in fig. 6. A laser beam incident from the left excites a second-order nonlinear crystal where parametric downconversion (PDC) occurs, leading to the generation of a pair of spatially entangled photons. One of these photons falls onto an object to be imaged. If it falls onto a low-loss region of the object, it will be transmitted and will be detected by the bucket detector shown in the figure. This detector provides no spatial information about the object. The other photon falls onto a photodetector array. This detector records the position of this photon and thus the position of the other photon in the plane of the object. By performing a coincidence measurement between these two measurements, one is able to determine the intensity structure of the object based on measurements of the properties of photons that have never physically interacted with the object. For this reason, this imaging method has been referred to as "ghost imaging".

There has been an ongoing discussion as to whether ghost imaging is a "quantum" phenomenon. The first demonstration of ghost imaging by Strekalov *et al.* [6] made

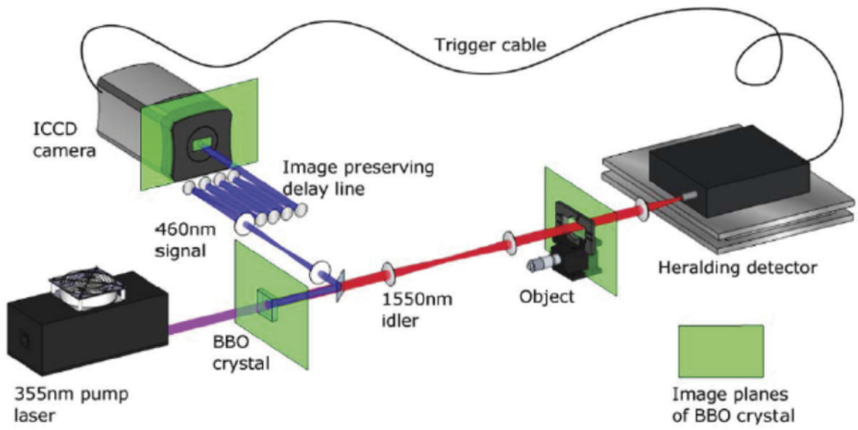

Fig. 7. – Setup for two-color ghost imaging. The BBO nonlinear crystal is designed to split pump photons at 350 nm into signal photons at 460 nm and idler photons at 1550 nm.

use of the correlations of entangled photons and certainly was quantum in this sense. However, the question was still open as to whether other types of correlations of a purely classical nature could be used to perform ghost imaging. One group [8] held that ghost imaging was a purely quantum effect. This claim was refuted by Bennink *et al.* (2002) [9] who reported the observation of ghost imaging through use of light beams that showed only classical correlations. The situation was clarified by the work of Gatti *et al.* [10], who developed a criterion for demonstrating quantum features of ghost imaging, namely the presence of correlations in both the near and far fields of the source of light source. These features were subsequently verified experimentally by Bennink *et al.* (2004) [12]. Specifically, they demonstrated that good ghost images were observed using the correlations of both the near and far fields of a parametric downconversion source, but that a classically correlated source could produce good ghost images in only one conjugate plane.

Aside from questions associated with the quantum or classical origin of ghost imaging, the fact remains that ghost imaging can provide new possibilities for image formation that are not available using traditional techniques. One example of such a modality is that of two-color ghost imaging. In this process, the light that illuminates the object can be of a significantly different wavelength of the light that falls onto the detector array. One achieves entanglement between two beams of very different wavelength by adjusting the orientation of the nonlinear crystal used to perform parametric downconversion to achieve phasematching for nondegenerate (different wavelength) conditions. An example of such a two-color ghost imaging measurement setup [19] is shown in fig. 7. A beta barium borate (BBO) nonlinear crystal is designed to split pump photons at 350 nm into signal photons at 460 nm and idler photons at 1550 nm. The 1550 nm photons fall onto the object, and the transmitted photons are registered by a sensitive "bucket" detector.

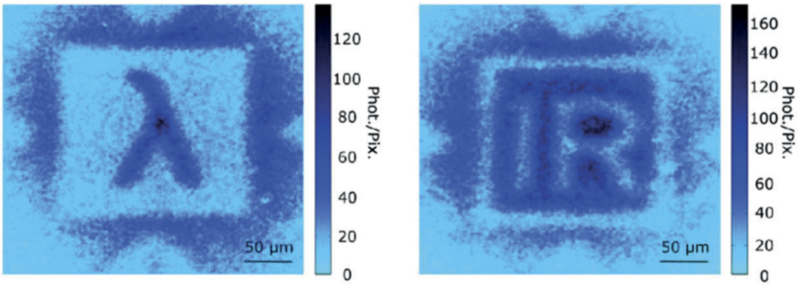

Fig. 8. – Ghost images recorded in the laboratory using the setup of fig. 7. The images show the properties of two stencils at a wavelength of 1550 nm, as recorded by a camera sensitive to 460 nm light. The objects are gold stencils on a silicon substrate.

This detector acts as a trigger for an imaging detector (labeled ICCD) that is sensitive to the 460 nm light. This trigger pulse must arrive approximately 50 ns before the image-bearing photon. These workers thus make use of an image-preserving delay line to ensure that the image-bearing photon arrives at the correct time. Some images obtained with this system are shown in fig. 8.

To summarize this section, we have seen that traditional ghost imaging is not an intrinsically quantum phenomenon, although some methods of ghost imaging can display quantum features. We will next turn to other sorts of quantum imaging that are intrinsically quantum in nature.

5. – Interaction-free imaging

In this section, we describe a quantum imaging procedure known as interaction-free imaging. Before we do so, let us first ask the question of what constitutes a quantum measurement. As a specific example, we consider the process shown in fig. 9. Here a single photon falls onto a beam splitter, and we wish to determine through which output port the photon leaves. In Situation 1, the detector to the right of the beam splitter registers the photon (the detector "clicks"). We thus know with certainty that the photon exited through the right-side output port of the beam splitter. Let us now consider the circumstance of Situation 2. In this case, the detector does not click. If we assume that the detector is ideal in that it registers every photon that falls onto it, we thereby conclude that the photon must have exited through the upper output port of the beam splitter. We thus reach the provocative conclusion that the lack of a detection event can constitute a quantum measurement. Similar situations have been described by Renninger [21] and by Dicke [22].

We next describe what is meant by an interaction-free measurement. The concept of an interaction-free measurement was introduced theoretically by Elitzur and Vaidman [23]. Interaction-free measurements were described experimentally by Kwiat *et al.* [24]. For conceptual clarity, we consider the situation described by White *et al.* [25]

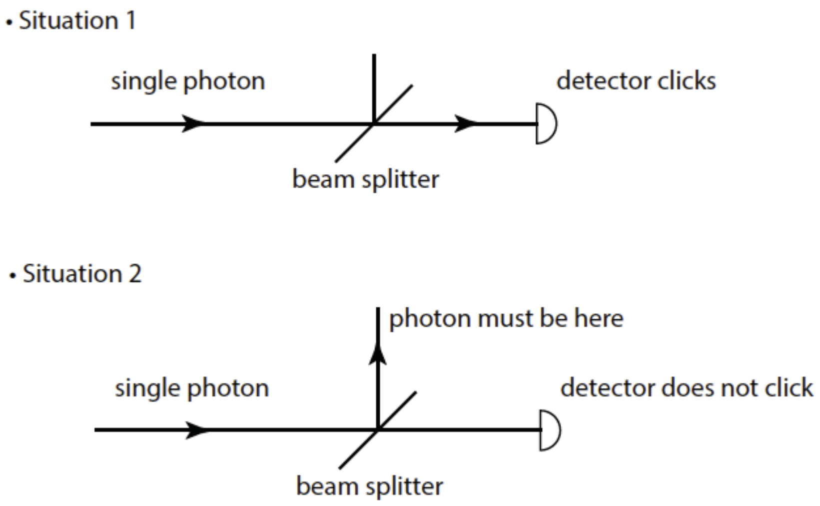

Fig. 9. – Even the lack of a detection event can constitute a quantum measurement.

as shown in fig. 10. Part a shows the situation in which a single photon falls onto a Mach-Zehnder interferometer in which the path lengths have been adjusted so that all light exits through the horizontal output port and falls onto detector D_1. Part b shows what happens if an opaque object is placed into the upper arm of the interferometer. The presence of this object blocks the upper path and thereby frustrates the destructive interference that prevented light from exiting through the port leading to detector D_2. Thus, 25% of the time the incident photon will fall onto D_2 and produce a click. This result is quite perplexing. It shows that one can deduce that an opaque object is located within the interferometer. However, we know that the photon did not physically strike the object, because the object is assumed to be opaque and we also know that the photon was detected by D_2. White *et al.* [25] developed this concept into a form of quantum imaging. They placed a focusing system into the upper arm of the interferometer and translated various objects through the focal region. In this way, they were able to map out the transmission profiles of these objects, as measured by photons that never directly interacted with the object.

6. – Imaging by Mandel's induced coherence

We next turn to another imaging modality, known as imaging by induced coherence. It is also known as imaging with undetected photons, as it was called in the original publication [26] demonstrating this effect. This procedure is fully quantum in nature.

As a first step, let us review the concept of induced coherence as described initially by the group of Mandel [27]. Their experimental setup is shown in fig. 11. Two parametric downconversion crystals NL1 and NL2 are pumped by a UV line of an argon ion laser. The signal beams from each crystal are combined at beam splitter BS_O, and the power

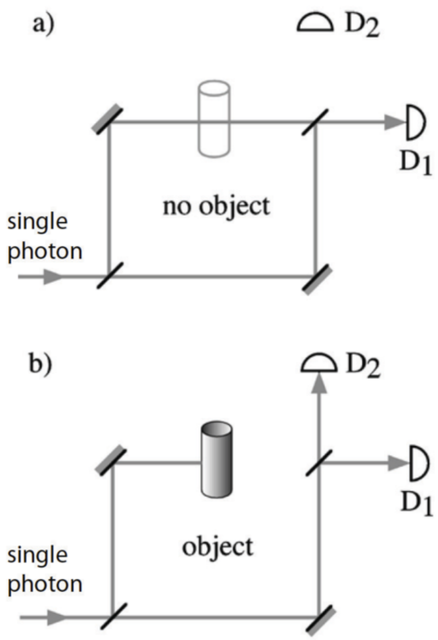

Fig. 10. – The concept of an interaction-free measurement. Adapted from White *et al.* [25] with permission.

hitting detector D_s is measured as a function of the position of BS_O as it is translated vertically. The results are shown in fig. 12. Interference fringes are observed when the idler beams from the two crystals are aligned (curve A). However, these fringes disappear when the idler beam path between the two crystals is blocked (curve B).

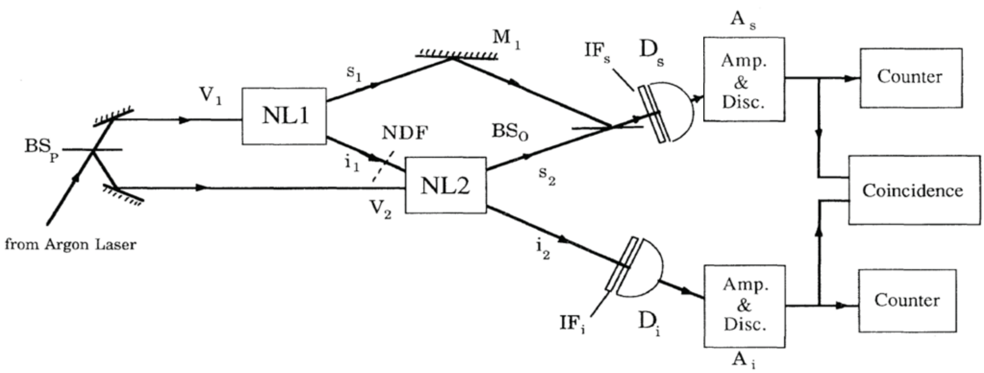

Fig. 11. – Setup for studying induced coherence [27], reproduced with permission.

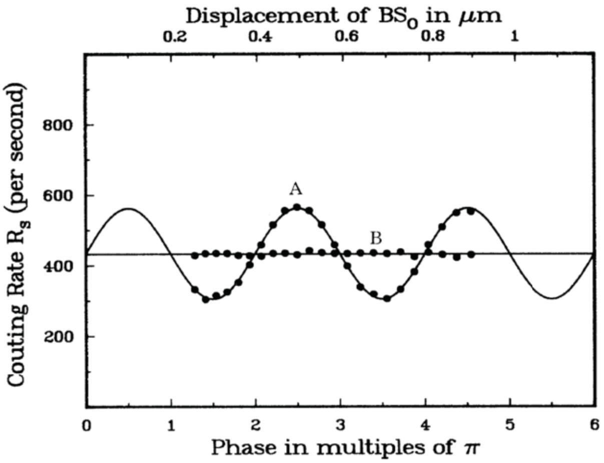

Fig. 12. – Results from the induced-coherence experiment of fig. 11. Curve A corresponds to the neutral density filter (NDF of fig. 11) having a transmission of 91%; curve B corresponds to the NDF having zero transmission.

These results are perhaps unexpected for the following reasons. In performing this measurement, the pump intensity was kept sufficiently low that there was essentially no *induced emission* from NL2. By this, one means, for example, that when the idler beam between the two crystals was blocked, the emission rate from NL2 did not change (decrease) by a measurable amount. Moreover, the emission rates from NL1 and NL2 were sufficiently low that there were essentially never photons from both NL1 and NL2 present simultaneously within the measure-ment device. Nonetheless, interference fringes were observed. The explanation of this effect is that interference occurs in quantum mechanics when two pathways are indistinguishable. Specifically, when the idler paths are unblocked and aligned, there is no way to tell if a photon arriving at D_s came from NL1 and NL2. Conversely, if a beam block is placed between the two crystals, then a "click" at D_i demonstrates that the photon pair was created in NL2. Thus, the pathways to Ds from NL1 and NL2 become distinguishable, and the interference no longer occurs.

These ideas were implemented in an imaging context by the group of Zeilinger in work published in 2014 [26]. Their experimental setup is shown in fig. 13. It is similar to that of fig. 11, except that an object O (the stencil of a cat) is placed in the pathway between NL1 and NL2. Also, the pump laser wavelength is 532 nm. The nonlinear crystals are cut for nondegenerate SPDC producing a signal photon at 810 nm and an idler photon at 1550 nm. D1 is a dichroic beamsplitter. The idler photon is directed along path d and the signal photon along path c. The image of the object O is thus impressed onto the idler photon, which is combined with the pump beam at D2 and both beams enter NL2 where another signal beam is created. The idler beam is then expelled from the setup at D3. The two signal beams from paths c and e are now combined at BS2 where

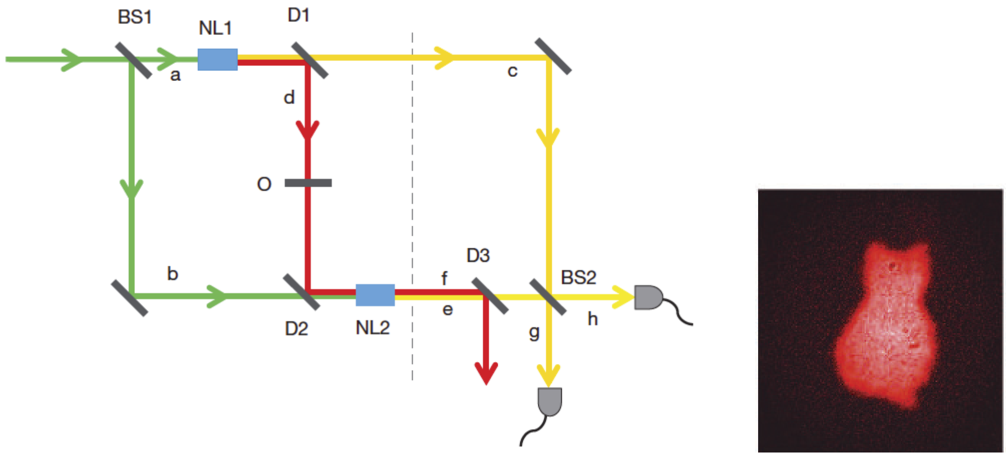

Fig. 13. – Left: Experimental setup to perform imaging based on induced coherence. Right: Image of a cat obtained with this experimental arrangement.

they interfere. The image of the cat, shown to the right of the figure, is created by the interference. As in the experiment of Mandel [27], the intensity of the idler beam in path d is too small to induce emission. Only the coherence of this beam is transferred to the signal beam in the process of PDC in NL2.

7. – Technology for quantum imaging

Significant technological progress has been made in recent years in the development of sensitive low-noise cameras. These cameras have properties that approach the ideal situation of a 100% detection quantum efficiency and a vanishing dark-count rate. Two of these modern cameras are as follows.

- Electron multiplied CCD (EMCCD) cameras have a detection quantum efficiency of about 80%, but have a background dark count rate of about 0.02 counts per pixel per readout. These specifications render these cameras suitable for many applications in quantum information.

- Intensified CCD (ICCD) cameras have a detection quantum efficiency of only about 20%, but can be gated in such a way that there are essentially no dark counts in an integration time. The ICCD camera was mentioned earlier in this chapter. It is the camera used in the work presented earlier in relation to fig. 7.

In the remainder of this section we describe the results of one particular study, that of Edgar *et al.* [28], which made use of an EMCCD camera. We note also the work of the group of Walmsley on similar topics [29]. To establish the context of the study of Edgar *et al.* [28], we present fig. 14, which shows the distribution of light produced by spontaneous parametric downconversion. Clearly the light is emitted into a very large

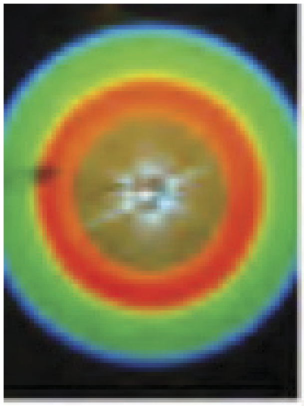

Fig. 14. – Spatial and spectral distribution of light generated by the process of spontaneous parametric downconversion (SPDC).

number of spatial and frequency modes of the field. Light emitted at opposite sides of the distribution are spatially entangled, for the reasons described in the description of fig. 5. Historically, one usually examined the nature of this entanglement through the use of point detectors that are raster-scanned through the intensity pattern. However, in the study of Edgar *et al.*, the entanglement of the entire distribution was measured simultaneously through use of an EMCCD camera.

The experimental setup of Edgar *et al.* [28] is shown in fig. 15. The pump source is a continuously running mode-locked Nd:YAG laser that is frequency tripled to produce an output at 350 nm. A BBO nonlinear crystal cut for type-I degenerate phase matching produces entangled photon pairs at 700 nm through the process of SPDC. In part (a) of the figure the plane of the BBO crystal is imaged onto the EMCCD to allow the measurement of correlations in position space. In part (b) the Fourier plane of the crystal is imaged onto the EMCCD to allow the measurement of correlations in transverse momentum. As spectral filter (not shown in the figure) centered at 700 nm with a bandwidth of 10 nm is placed immediately in front of the camera so that only photons of nearly the same wavelength were detected.

Some of the results of this study are shown in fig. 16. The panel on the left shows that there is a strong correlation in the spatial positions of the signal and idler photons. The panel on the right shows that there is a strong anticorrelation between the momenta of the signal and idler photons. Strong correlations in either position or momentum (whichever one chooses to measure) is the key signature of quantum entanglement. This thought can be rendered quantitative in terms of the Reid criterion which states that

$$\Delta^2_{\min}(x_1|x_2)\ \Delta^2_{\min}(p_{x1}|p_{x2}) > \frac{\hbar^2}{4}\,,$$

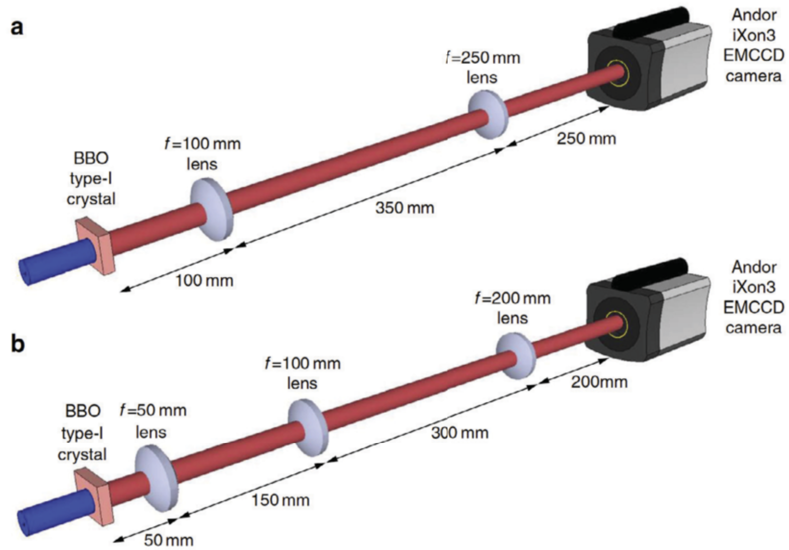

Fig. 15. – Experimental scheme used to measure (a) position and (b) momentum correlations. In (a) the camera is in an image plane of the PDC crystal; in (b) it is in the Fourier plane of the crystal.

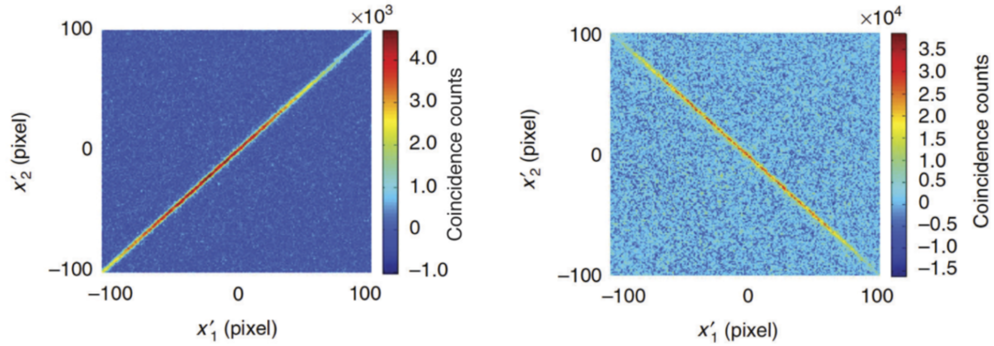

Fig. 16. – Probability distributions for joint detections in the image plane (left) and far-field (right).

where $\Delta^2_{\min}(r_1|r_2)$ is the minimum inferred variance, describing the minimum uncertainty in measuring the variable r_1 conditional on the measurement of variable r_2. The violation of this inequality is a signature of entanglement. Edgar *et al.* [28] report an uncertainty product of

$$\Delta^2_{\min}(x_1|x_2)\ \Delta^2_{\min}(p_{x1}|p_{x2}) > 6 \times 10^{-4}\hbar^2,$$

which is an indication of strong entanglement. Edgar *et al.* also estimate that there are 2500 spatial modes of the light field that are entangled.

8. – Summary and discussion

Quantum imaging is a still-developing field with important implications. Quantum methods can be used to form images that are better than classical images in terms of sensitivity and spatial resolution. From a different perspective, imaging methods can be used the enhance the protocols of quantum information. Image science is capable of exploiting the parallelism that is intrinsic to many of the procedures of quantum information science. One example is the simultaneous entanglement involving a very large number of modes of the optical field [28, 30].

In this paper, we have presented a broad overview of quantum imaging, while concentrating on several imaging protocols of current research interest. Three different examples of quantum imaging are described, namely ghost imaging, imaging based on interaction-free measurements, and imaging based on Mandel's induced coherence.

REFERENCES

[1] KOLOBOV M., (Editor) *Quantum Imaging* (Springer-Verlag New York) 2007.
[2] ANDERSON U. L., GEHRING T., MARQUARDT C. and LEUCHS G., *Phys. Scripta*, **91** (2016) 053001.
[3] SLUSHER R., HOLLBERG L., YURKE B. and MERTZ J., in *Optical Instabilities, Proceedings of the International Meeting on Instabilities and Dynamics of Lasers and Nonlinear Optical Systems, University of Rochester, June 18-21, 1985*, edited by BOYD R. W., RAYMER M. G. and NARDUCCI L. M. (Cambridge University Press); see also SLUSHER R., HOLLBERG L., YURKE B., MERTZ J. and VALLEY J., *Phys. Rev. Lett*, **55** (1985) 2409.
[4] XIAO M., WU L. A. and KIMBLE H. J., *Phys. Rev. Lett.*, **59** (1987) 278.
[5] SOUTO RIBEIRO P. H., SCHWOB C., MAÎTRE A. and FABRE C., *Opt. Lett.*, **24** (1997) 1893.
[6] STREKALOV D. V., SERGIENKO A. V., KLYSHKO D. N. and SHIH Y. H., *Phys. Rev. Lett.*, **74** (1995) 3600.
[7] PITTMAN T. B., SHIH Y. H., STREKALOV D. V. and SERGIENKO A. V., *Phys. Rev. A*, **52** (1995) R3429.
[8] ABOURADDY A. F., SALEH B. E. A., SERGIENKO A. V. and TEICH M. C., *Phys. Rev. Lett.*, **87** (2001) 123602.
[9] BENNINK R. S., BENTLEY S. J. and BOYD R. W., *Phys. Rev. Lett.*, **89** (2002) 113601.
[10] GATTI A., BRAMBILLA E. and LUGIATO L. A., *Phys. Rev. Lett.*, **90** (2003) 133603.
[11] GATTI A., BRAMBILLA E., BACHE M. and LUGIATO L. A., *Phys. Rev. Lett.*, **93** (2003) 093602.
[12] BENNINK R., BENTLEY S. J., BOYD R. W. and HOWELL J. C., *Phys. Rev. Lett.*, **92** (2004) 033601.
[13] O'SULLIVAN M. N., CHAN K. W. C. and BOYD R. W., *Phys. Rev. A B*, (2010) 053803.
[14] CHAN K. W. C., O'SULLIVAN M. N. and BOYD R. W., *Opt. Express*, **18** (2010) 5562.
[15] ZEROM P., SHI Z., O'SULLIVAN M. N., CHAN K. W. C., KROGSTAD M., SHAPIRO J. H. and BOYD R. W., *Phys. Rev. A*, **86** (2012) 063817.

[16] TASCA D. S., ASPDEN R. S., MORRIS P. A., ANDERSON G., BOYD R. W. and PADGETT M. J., *Optics Express*, **21** (2013) 30460.
[17] ASPDEN R. S., TASCA D. S., BOYD R. W. and PADGETT M. J., *New J. Phys.*, **15** (2013) 073032.
[18] ASPDEN R. S., TASCA D. S., FORBES A., BOYD R. and PADGETT M. J., *J. Mod. Optic.*, (2014) `http://dx.doi.org/10.1080/09500340.2014.899645`.
[19] ASPDEN R. S., GEMMELL N. R., MORRIS P. A., TASCA D. S., MERTENS L., TANNER M. G., KIRKWOOD R. A., RUGGERI A., TOSI A., BOYD R. W., BULLER G. S., HADFIELD R. H. and PADGETT M. J., *Optica*, **2** (2015) 1049.
[20] MORRIS P. A., ASPDEN R. S., BELL J. E. C., BOYD R. W. and PADGETT M. J., *Nat. Commun.*, **6** (2015) 5913.
[21] RENNINGER M., *Z. Phys.*, **15S** (1960) 417.
[22] DICKE R. H., *Am. J. Phys.*, **49** (1981) 925.
[23] ELITZUR A. and VAIDMAN L., *Found. Phys.*, **23** (1993) 987; see also VAIDMAN L., *Quant. Opt.*, **6** (1994) 119.
[24] KWIAT P., WEINFURTER H., HERZOG T., ZEILINGER A. and KASEVICH M. A., *Phys. Rev. Lett.*, **74** (1995) 4763.
[25] WHITE A. G., MITCHELL J. R., NAIRZ O. and KWIAT P. G., *Phys. Rev. A*, **58** (1998) 605.
[26] BARRETO LEMOS G., BORISH V., COLE G. D., RAMELOW S., LAPKIEWICZ R. and ZEILINGER A., *Nature*, **512** (2014) 409.
[27] ZOU X. Y., WANG L. J. and MANDEL L., *Phys. Rev. Lett.*, **6** (1991) 318.
[28] EDGAR M. P., TASCA D. S., IZDEBSKI F., WARBURTON R. E., LEACH J., AGNEW M., BULLER G. S., BOYD R. W. and PADGETT M. J., *Nat. Commun.*, (2012) DOI: 10.1038/ncomms1988.
[29] ZHANG L., NEVES L., LUNDEEN J. S. and WALMSLEY I. A., *J. Phys. B*, **42** (2009) 114011.
[30] O'SULLIVAN-HALE M. N., ALI KHAN I., BOYD R. W. and HOWELL J. C., *Phys. Rev. Lett.*, **94** (2005) 220501.